Since January 2020 Elsevier has created a COVID-19 resource centre with free information in English and Mandarin on the novel coronavirus COVID-19. The COVID-19 resource centre is hosted on Elsevier Connect, the company's public news and information website.

American Journal of Otolaryngology–Head and Neck Medicine and Surgery 42 (2021) 102970

Contents lists available at ScienceDirect

American Journal of Otolaryngology–Head and Neck Medicine and Surgery

journal homepage: www.elsevier.com/locate/amjoto

Aerosol and droplet generation from orbital repair: Surgical risk in the pandemic era

Michael J. Ye [a,*,1], Raghav B. Vadhul [b,1], Dhruv Sharma [a], Vincent J. Campiti [b], Sarah J. Burgin [a], Elisa A. Illing [a], Jonathan Y. Ting [a], Jae Hong Park [c], Karl R. Koehler [d], Hui Bae Lee [e], Dominic J. Vernon [a], Jeffrey D. Johnson [a], B. Ryan Nesemeier [f], Taha Z. Shipchandler [a]

[a] Indiana University Department of Otolaryngology – Head and Neck Surgery, USA
[b] Indiana University School of Medicine, USA
[c] School of Health Sciences, Purdue University, West Lafayette, IN, USA
[d] Boston Children's Hospital, Harvard Medical School, Department of Otolaryngology – Head and Neck Surgery, USA
[e] Indiana University Department of Ophthalmology, USA
[f] The Ohio State University Department of Otolaryngology – Head and Neck Surgery, USA

ARTICLE INFO

Keywords:
COVID-19
Coronavirus
Surgery
Facial trauma
Orbit
Orbital rim
Otolaryngology
Oculoplastics
Ophthalmology
Plastic surgery
Maxillofacial
Droplet
Splatter
Aerosol
Drill
Smoke
Plume

ABSTRACT

Introduction: The highly contagious COVID-19 has resulted in millions of deaths worldwide. Physicians performing orbital procedures may be at increased risk of occupational exposure to the virus due to exposure to secretions. The goal of this study is to measure the droplet and aerosol production during repair of the inferior orbital rim and trial a smoke-evacuating electrocautery handpiece as a mitigation device.

Material and methods: The inferior rim of 6 cadaveric orbits was approached transconjunctivally using either standard or smoke-evacuator electrocautery and plated using a high-speed drill. Following fluorescein inoculation, droplet generation was measured by counting under ultraviolet-A (UV-A) light against a blue background. Aerosol generation from 0.300–10.000 μm was measured using an optical particle sizer. Droplet and aerosol generation was compared against retraction of the orbital soft tissue as a negative control.

Results: No droplets were observed following the orbital approach using electrocautery. Visible droplets were observed after plating with a high-speed drill for 3 of 6 orbits. Total aerosol generation was significantly higher than negative control following the use of standard electrocautery. Use of smoke-evacuator electrocautery was associated with significantly lower aerosol generation in 2 of 3 size groups and in total. There was no significant increase in total aerosols associated with high-speed drilling.

Discussion and conclusions: Droplet generation for orbital repair was present only following plating with high-speed drill. Aerosol generation during standard electrocautery was significantly reduced using a smoke-evacuating electrocautery handpiece. Aerosols were not significantly increased by high-speed drilling.

1. Introduction

As the highly contagious coronavirus disease 2019 (COVID-19) pandemic continues, resulting in tens of millions infections and more than three hundred thousand deaths in the United States alone [1], the defining question within healthcare is how to continue delivering care in a manner that is safe for both patients and providers. While mitigation strategies, such as mask wearing and symptom screenings, are thought to be efficacious at limiting spread from major modes of COVID-19 transmission including droplets [2,3] and aerosols [4,5], there remains a great deal of uncertainty about particle generation and risk mitigation in the surgical setting. This led the Centers for Disease Control and Prevention and other worldwide health organizations to recommend temporarily halting elective procedures during the start of the pandemic to limit spread of the virus [6]. Among those at increased risk for occupational exposure to the virus may be physicians who perform

* Corresponding author at: Department of Otolaryngology – Head and Neck Surgery, Indiana University School of Medicine, 1130 W. Michigan Street, Suite 400, Indianapolis, IN 46202, USA.
E-mail address: mjye@iu.edu (M.J. Ye).
[1] Contributed equally to this work.

https://doi.org/10.1016/j.amjoto.2021.102970
Received 21 January 2021;
Available online 27 February 2021

orbital procedures, as the SARS-CoV-2 virus has been isolated from the ocular surface of infected patients [7] and due to exposure to nasal and oral secretions [8].

This is especially pertinent in the field of orbital trauma, due to the potential for asymptomatic carriers [9] and because often surgical repair cannot be deferred until resolution of an active infection without detriment to the patient [10–13]. Additionally, these procedures which commonly employ electrocautery and high speed drills in close proximity to the mucous membranes of the eye [8] are suspected to be droplet and aerosol generating, placing providers at increased risk [14].

Due to these reasons, there is a critical need for data to guide the safety policy surrounding these procedures. Despite this, there are no studies to date quantifying the droplet and aerosol generation from orbital fracture repair. In order to close this information gap, this cadaveric simulation was devised to measure the generation of droplets and aerosols from inferior orbital rim repair and trial the use of a smoke evacuating electrocautery device as a particulate mitigation device.

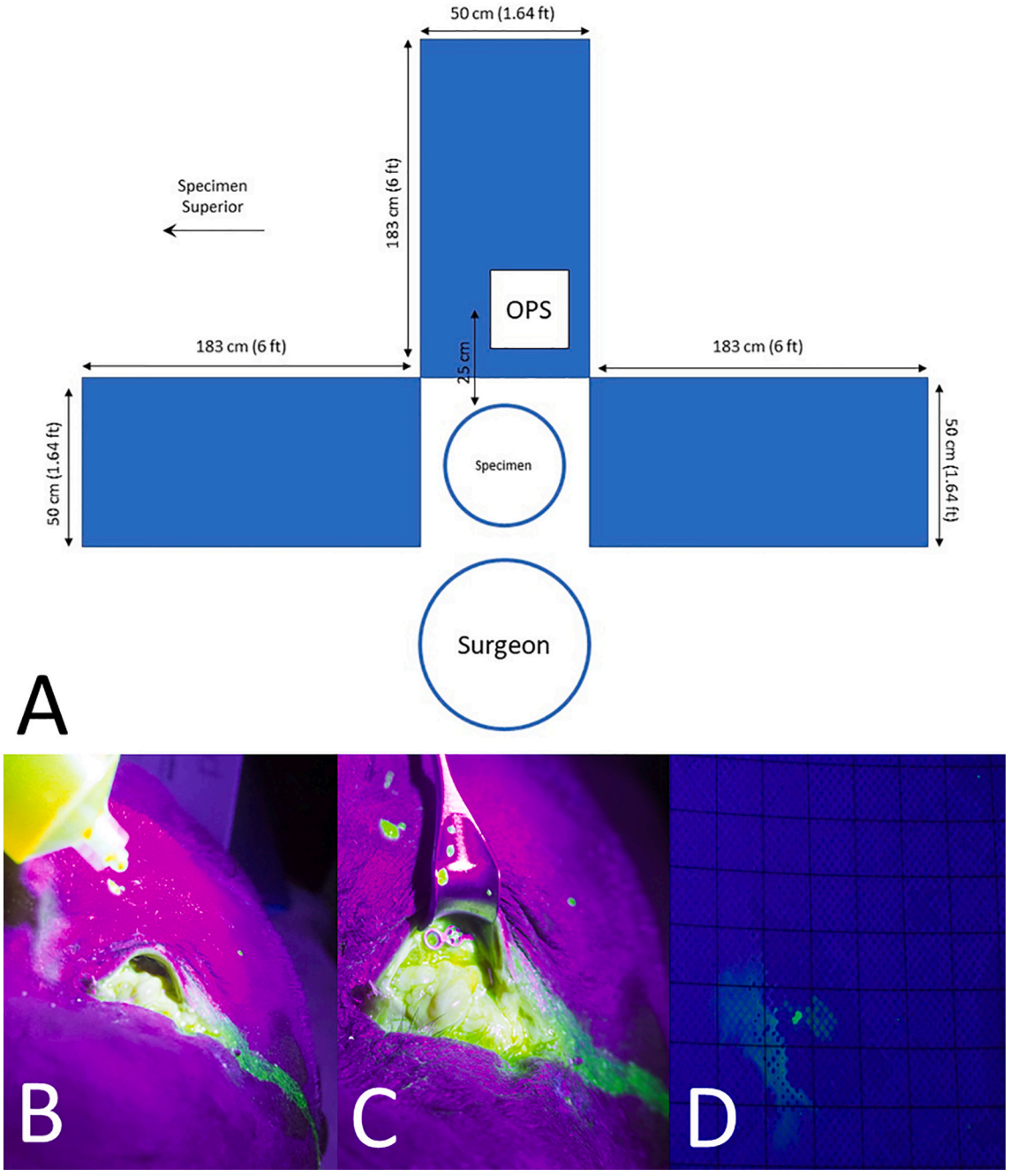

Fig. 1. A) Schematic of experimental setup. Impermeable blue papers were affixed to three 183 cm × 50 cm boards and to a 25 cm × 25 cm area of the surgeon's chest. The optical particle sizer (OPS) was positioned 25 cm away from each surgical site. B) Photograph of orbital surgical site under ultraviolet-A (UV-A) light showing broad fluorescein positivity and the syringe and fluorescein solution used for irrigation during powered drilling. C) Photograph of postoperative orbital surgical site under UV-A light showing broad fluorescein positivity and plate in place. D) Representative photograph of fluorescein splatter under ultraviolet-A (UV-A) light with overlayed 1 × 1 cm transparent plastic grid.

2. Material and methods

2.1. Supplies and equipment

This study was exempt from institutional review board due to the use of non-living deidentified human cadaveric tissue specimens (IRB protocol # 2004100753). Three fresh-frozen cadaveric head specimens were used for the experiments conducted in this study, and all experiments were performed in a dedicated surgical laboratory as described in the "Surgical technique" section below. Data from incision to exposure of the orbital rim and floor and from plating were taken as separate experimental conditions and referred to as "approach" and "plating" respectively. Between experimental conditions, a high-efficiency particulate air (HEPA) filtration system was utilized until aerosol levels returned to baseline.

2.2. Droplet measurement

Each cadaver head was placed in the standard supine position for orbital floor repair surgery oriented such that the operative orbit was closest to the surgeon. Three sheets of nonabsorbent blue paper measuring 183 cm (6 ft) × 50 cm (1.64 ft) were affixed to a rigid backing and were placed 90° from each other in the following directions: (1) surgeon left, (2) across from the surgeon, and (3) surgeon right (Fig. 1). The surgeon's surgical gown was also affixed with a 25 cm × 25 cm piece of nonabsorbent blue paper on the chest, and a face shield was worn throughout the procedure.

Fluorescein was utilized in droplet measurement as it fluoresces yellow under ultraviolet-A (UV-A) light while the blue background does not. This is an established method for measuring droplet production from surgical procedures and reliably detects droplets in the submillimeter and greater range [15–17]. The specimens were prepared through inoculation using a 1 mg/mL fluorescein solution created with 10% fluorescein injection (USP; AK-Fluor) and sterile saline. 2 mL of the fluorescein solution were injected transconjunctivally into each orbit through a 25-gauge hypodermic needle by advancing the needle until orbital rim was palpated. The needle was then walked along the rim and superiorly to the floor, injecting at each location, and finally retracted while injecting until the needle was fully withdrawn. Broad positivity was confirmed for each surgical site under ultraviolet-A (UV-A) light (Fig. 1b & c).

Prior to each experimental condition, all surfaces were inspected under UV-A light for fluorescein and cleansed of any droplets. The size, number, and distance of droplets were measured on nonabsorbent blue paper placed around the cadaver head following each surgical procedure. Transparent 25 cm × 25 cm transparent grids were laid side-by-side until the entire paper was covered. The blue papers affixed to the surgeon's chest and the face shield were evaluated in the same manner as well. The number of 1 cm × 1 cm squares containing fluorescein positivity was counted for each procedure as recorded as the droplet count (Fig. 1d). The size and travel-distance of droplets were measured using a ruler.

2.3. Aerosol sampling

An optical particle sizer (OPS 3330; TSI Inc.) was employed to monitor aerosol particle concentration from 0.300 to 10.000 μm distributed across 16 intervals as depicted on the x-axis of Fig. 3a. The sampling flow rate was set at 1.0 L/min through the 3 mm intake port positioned 25 cm away from the surgical site, directly across from the surgeon (Fig. 1). Measurements were recorded on a second-by-second basis throughout the duration of each procedure. A 60-second baseline was measured prior to the start of each condition.

2.4. Surgical technique

All procedures were performed by a fellowship trained facial plastic surgeon with an assistant providing retraction. A transconjunctival preseptal swinging eyelid approach was used to approach the orbit. The lateral canthotomy and inferior cantholysis were performed using sharp dissection. Monopolar electrocautery on "cut" was used to make the transconjunctival incision and dissect in the preseptal plane until reaching the inferior orbital rim. Monopolar electrocautery set to coagulation mode was then used to divide the periosteum at the arcus marginalis. This was performed using a standard monopolar electrocautery hand piece for orbits 1, 2, and 3 and a smoke-evacuating hand piece for orbits 4, 5, and 6. A Cottle elevator was used to dissect in a subperiosteal plane to expose adequate orbital floor and rim for implant placement and plating. A curvilinear 4–0 0.8 mm plate was fixed to the orbital rim using the powered drill (Stryker CORE Micro Drill with 5 mm midface drill at 40,000 rotations per minute) and screws while irrigating with a solution of 1 mg/mL fluorescein in saline. Negative controls were obtained by measuring aerosols during retraction of the inferior lid for 60 s compared to a 60-second pre-retraction baseline.

2.5. Statistical analysis of aerosol data

All statistical analyses were performed using the Statistical Package for Social Sciences (IBM SPSS Statistics for Windows, Version 26.0; IBM Corp.). Data collected during electrocautery use was excluded from analysis due to electrical interference resulting in intermittent read errors from the OPS. The average concentration of particles in each of the size distributions ranging from 0.300–10.000 μm was calculated and compared to the baseline. These sizes were categorized into small (0.300–0.897 μm), medium (0.898–2.685 μm), large (2.686–10.000 μm), and total (0.300–10.000 μm).

Aerosol generation was defined as a change in particle number concentration compared to baseline. Statistical comparisons were performed between the different experimental conditions and the negative control. Additional analysis was performed comparing aerosol generation for 30 s before initation of electrocautery and 30 s after cessation for both standard and smoke-evacuating electrocautery. Drill aerosol generation analysis was performed by comparing particle counts for the 30 s prior to the first use of the drill, during drilling, and for 30 s after the last use of the drill. These measurements were compared to the negative control to determine statistical significance. All inferential statistics were performed with Mann-Whitney-*U* tests, and statistical significance was determined with an alpha value of 0.05.

3. Results

3.1. Droplet analysis

No droplets were produced for any of the approach conditions. Visible droplets were observed under UV-A light following plating of the inferior rim on orbits 1, 3, and 6 (Table 1). For orbit 1, four droplets were noted between 15 and 18 cm from the surgical site to surgeon left and measured <1 mm in diameter. For orbit 3, five droplets were produced to the surgeon right, two to surgeon left, and one on the surgeon's chest. The droplets on the right were located 30.5 cm, 30.5 cm, 33 cm, 48.3 cm, and 66.8 cm from the surgical site. Two of these were 1 mm in diameter, and the remaining 3 were <1 mm in diameter. Following the plating of orbit 6, two droplets were noted across from the surgeon at 30.5 cm and 41.9 cm from the surgical site measuring <1 mm. The farthest travel-distance measured was 66.8 cm to the surgeon right. Fluorescein-positivity was observed on used surgical instruments and on the specimen itself following each experimental condition (Fig. 1b/c). No droplets were observed following each of the negative control conditions.

Table 1
Droplet generation following approach and plating for orbital rim repair.

Droplet splatter results						
Orbit	Procedure	Droplet contamination	Location	Number of droplets	Distance from surgical site, cm	Maximum droplet size, mm
1	Approach	No	–	–	–	–
	Plating	Yes	Surgeon left	4	15–18	<1
2	Approach	No	–	–	–	–
	Plating	No	–	–	–	–
3	Approach	No	–	–	–	–
	Plating	Yes	Surgeon right, left, chest	7	30.5–66.8	<1–1
4	Approach	No	–	–	–	–
	Plating	No	–	–	–	–
5	Approach	No	–	–	–	–
	Plating	No	–	–	–	–
6	Approach	No	–	–	–	–
	Plating	Yes	Surgeon across	2	30.5, 41.9	<1

3.2. Aerosol generation

Across 6 orbits, aerosol concentrations during surgical approach utilizing standard electrocautery were significantly higher than negative control in all three size groups ($p \leq 0.010$) (Table 2). This was also true for small, medium, and total particle concentrations following the use of smoke-evacuator electrocautery ($p < 0.001$), but not large particle concentrations ($p = 0.732$), where the amounts measured were significantly less in 2 of 3 size categories and in total compared to approach with the standard electrocautery hand piece (Fig. 2a). During plating, the concentrations of small, medium, large, or total aerosols produced were not significantly different from negative control ($p = 0.456$, 0.264, 0.366, 0.619) (Fig. 2b).

The majority of aerosol particles produced throughout all procedures were in the small size range, specifically 0.300–0.374 μm. On visual inspection of line graphs depicting aerosol generation over time for these procedures, there appeared to be spikes in concentration following electrocautery and drilling (Fig. 3a/b/c), so a comparison of aerosol counts following electrocautery use to a pre-electrocautery baseline was performed. There was a significant increase in total aerosols following electrocautery using a standard hand piece (mean = 29.989 particles/cm^3, $p < 0.001$) and smoke-evacuating electrocautery (mean = 1.468 particles/cm^3, $p = 0.007$) with significantly lower aerosol generation associated with use of the smoke-evacuating handpiece ($p < 0.001$). A small but not statistically significant increase in aerosol particle number was detected during drilling (mean = 0.332 particles/cm^3, $p = 0.096$) and during the 30 s immediately following drilling (mean = 0.600 particles/cm^3, $p = 0.077$) (Fig. 3d).

4. Discussion

The rapidly spreading and deadly COVID-19 has infected more than 90 million people worldwide [1]. Due to the potential for nosocomial spread through droplet and aerosol generating procedures, numerous organizations recommended halting elective medical procedures during the height of the pandemic [6]. As medical systems around the world continue to remobilize and devise strategies for safely performing these procedures, there has been a flurry of activity to quantify the risk of surgical instrumentation of upper aerodigestive tract mucosal surfaces and investigate the efficacy of mitigation strategies. The existing literature largely focuses on endonasal procedures [15,17]. However, there has been little to no objective measurement of droplet and aerosol production after orbital surgery, despite evidence that the ocular surface can harbor SARS-CoV2 virions [7] and the risk of direct contact with the mucous membranes of the eye [8,18,19]. In order to close this gap, this study presents a quantification of droplet and aerosol production during surgical repair of the inferior orbit rim.

Droplet production was not seen following the transconjunctival orbital floor approach for any of the 6 surgical sites. However, there were visible droplets after plating for 3 of 6 orbits. This suggests that plating and powered drilling with irrigation poses the highest risk of droplet splatter during orbital rim repairs—more so than electrocautery. Workman et al. recently demonstrated high droplet production with the use of a high-speed drill in endonasal procedures, and several previous orthopedic studies have shown similar results with the use of a drill as well [17,20–23]. This does however contrast with previous work done by our group showing that mandible and midface repair via sublabial approach was not droplet-producing [24]. This difference may be due to the lips and soft tissue acting as a barrier to droplets when a sublabial approach is used. In comparison, drilling at the orbital rim is more superficial with fewer anatomic features to block splatter. This principle may be applicable to other areas where powered instrumentation is used, but further investigation is warranted prior to drawing definitive conclusions.

Aerosol sampling demonstrated significant aerosol generation during transconjunctival orbital floor approach in the majority of size ranges measured, regardless of whether standard or smoke-evacuator electrocautery was used. However, the approach using smoke-evacuator electrocautery was significantly less aerosol generating than the approach using standard electrocautery. Analysis of total particle counts before and after use of electrocautery compared to negative control similarly showed a significant increase in total particle number concentration associated with standard monopolar electrocautery ($p <$ 0.001) and with the smoke evacuating electrocautery hand piece ($p =$

Table 2
Average aerosol particle concentration over baseline for each procedure. (*)-Denotes statistical significance from negative control ($p < 0.05$). n = 6 for all conditions.

	Average aerosol particle concentration over baseline (particles/cm^3)			
	Small (0.300–0.897 μm)	Medium (0.898–2.685 μm)	Large (2.686–10.000 μm)	Total (0.0300–10.000 μm)
Standard electrocautery approach	11.57* ($p < 0.001$)	0.82* ($p < 0.001$)	0.15* ($p = 0.01$)	12.54* ($p < 0.001$)
Smoke-evacuator electrocautery approach	1.93* ($p < 0.001$)	0.10* ($p < 0.001$)	0.10 ($p = 0.732$)	2.13* ($p < 0.001$)
Plating	0.58 ($p = 0.456$)	0.01 ($p = 0.264$)	0.00 ($p = 0.366$)	0.60 ($p = 0.619$)
Negative control	0.43	0.00	0.00	0.42

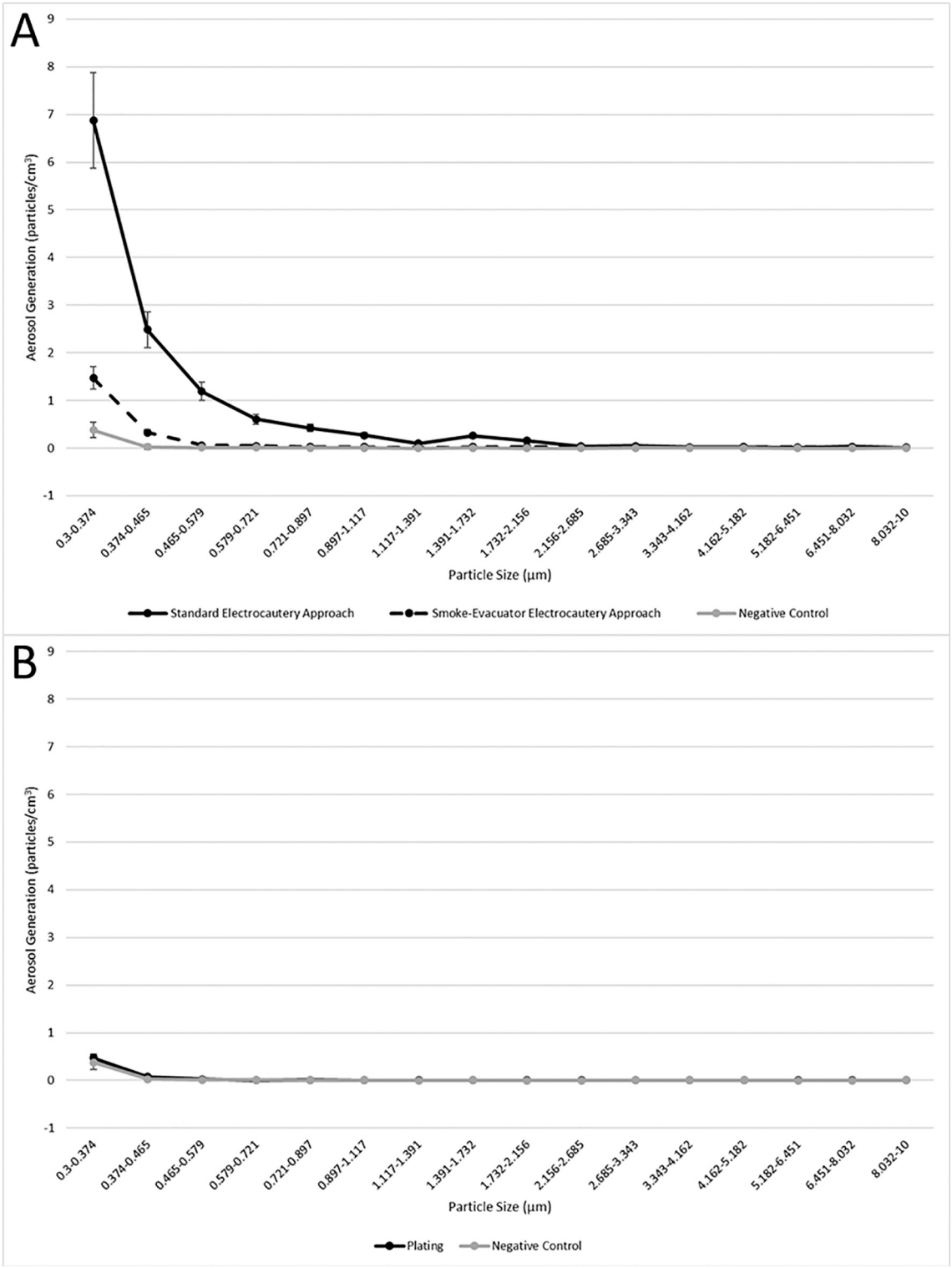

Fig. 2. A) Average aerosol generation by size measured during approach with standard electrocautery, approach with smoke-evacuator electrocautery, and negative control. Error bars represent 95% confidence intervals. Aerosol generation was defined by change in particle number concentration over baseline. B) Average aerosol generation by size measured during plating and negative control. Error bars represent 95% confidence intervals.

0.007). However, the smoke evacuating handpiece was associated with a 95.1% reduction in aerosol generation ($p < 0.001$). Previous studies of smoke-evacuation systems have provided similar results in regards to limiting the production and spread of aerosols [17,25].

The majority of aerosols produced was in the small (0.300–0.897 µm) range. SARS-CoV-2 virions are estimated to range between 0.07 and 0.09 µm in diameter based on transmission electron microscopy data, and other viruses from the same family have a diameter of around 0.05–0.150 µm [26,27] and could be carried by particles in this size range. In light of these results, the authors recommend continued use of enhanced personal protective equipment (PPE) including N95 or powered air purifying respirator (PAPR) for these operations. Use of self-

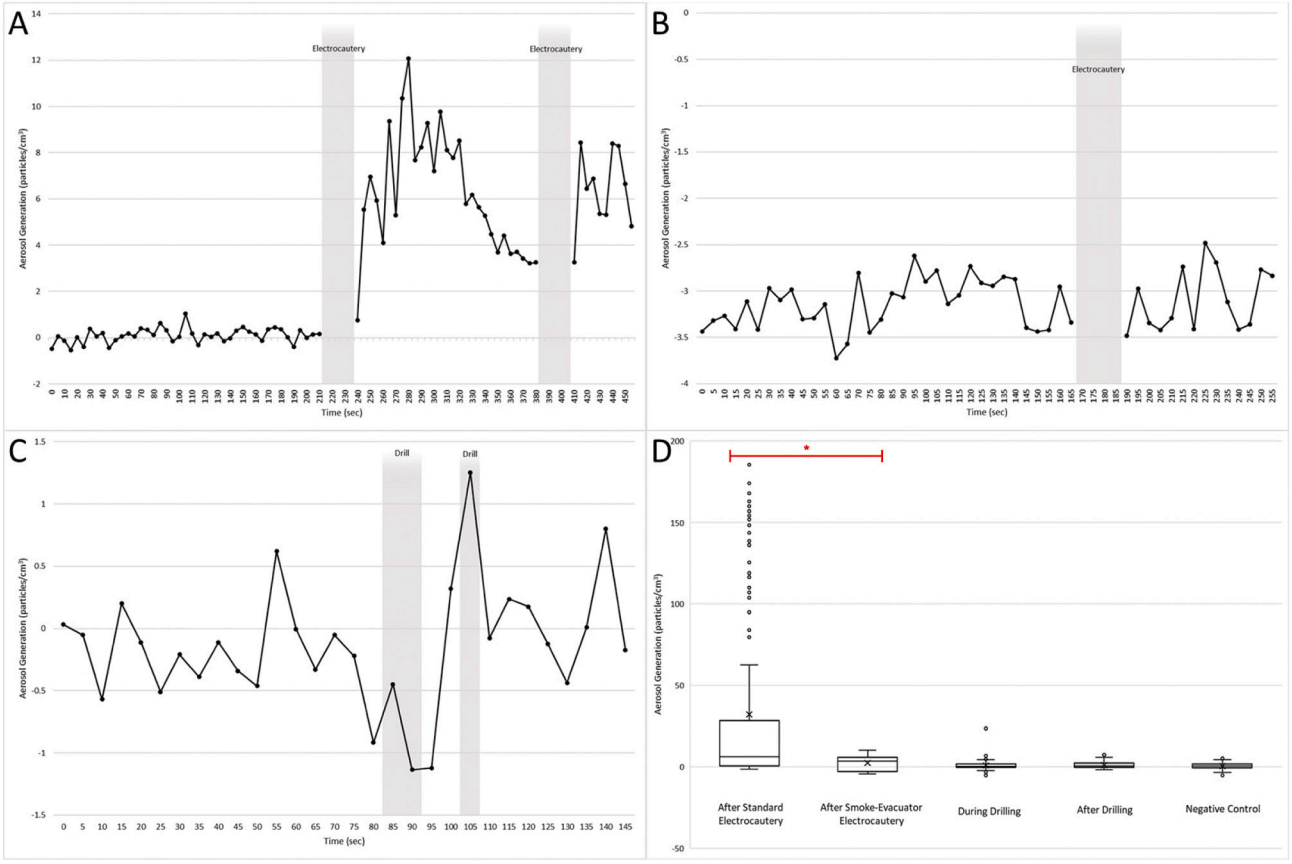

Fig. 3. A) Aerosol generation during a representative transconjunctival approach to the inferior orbital rim repair using standard electrocautery. Shaded areas represent electrocautery use, with excluded data points due to electrical interference with optical particle sizer. Aerosol generation was defined by change in particle number concentration over baseline. B) Aerosol generation during a representative approach to the inferior orbital rim repair using the smoke evacuating electrocautery hand piece. Shaded areas represent electrocautery use, with excluded data points due to electrical interference with optical particle sizer. C) Aerosol generation during plating. Shaded areas represent high-speed drilling. D) Box and whisker plot depicting aerosol generation from standard electrocautery (n = 4), smoke-evacuator electrocautery (n = 3), during drilling (n = 12), and after drilling (n = 12). 95% confidence intervals are shown. Asterisk denotes statistically significant difference between aerosol generation from standard versus smoke-evacuating electrocautery ($p < 0.001$). Statistically significant increases in aerosols resulted from standard ($p < 0.001$) and smoke-evacuating electrocautery ($p = 0.007$) use but not from the other conditions when compared to the negative control.

drilling screws and other non-powered instrumentation instead of powered drills may limit droplet production. Clear plastic drape systems have also been used effectively to reduce droplets from a variety of head and neck procedures [28–30]. In addition, preoperative screening and testing for COVID-19 may help guide decision making where resources permit.

Plating did not produce significantly more aerosols than negative controls. This is a somewhat surprising result considering the established literature demonstrating aerosol generation from orthopedic [31] and endonasal drilling [15,17]. This may be due to the comparatively smaller caliber drill and short duration of activation. The data also demonstrates that drilling is droplet-producing, but not aerosol-generating, which may suggest a low correlation between droplet and aerosol production. These findings are corroborated in a recent study by Guderian et al., which similarly demonstrated that drilling generates fewer aerosol particles than electrocautery [32]. Other recent literature shows little to no aerosol generation from drilling with irrigation during mandible and midface fixation [24,33].

Several limitations of this study warrant discussion. Only droplets that were visible to the naked eye were recorded. And, only the cardinal directions were examined for droplets, leaving out potential spread in a full 360° arc. The OPS only measured particles in the 0.300–10.000 μm range and was placed at a fixed location 25 cm across from the surgeon. This may only reflect the exposure to surgeons and surgical technologists. Future studies are necessary to quantify aerosol levels at the distance of the average anesthesiologist and circulating staff. This study was also performed on a cadaver head, which may differ from living patients due to temperature and blood flow. Lastly, we did not specifically study the presence of viral particles or their properties.

5. Conclusions

During cadaveric orbital repair, the transconjunctival approach using sharp dissection and electrocautery was not droplet-producing. However, visible droplets were seen after plating using a powered drill in three of six orbital rim repair operations (50%). Aerosol particle measurement in the 0.300–10.000 μm range revealed an increase in concentration after electrocautery use ($p \leq 0.010$). The use of a smoke evacuating electrocautery handpiece was effective at reducing aerosol generation when compared to standard electrocautery. Powered drilling was not significantly aerosol generating.

Funding source

Self-funded.

CRediT authorship contribution statement

Michael J. Ye, MD, Raghav B. Vadhul BS - Experimental design, IRB application, materials acquisition, subject recruitment, data collection,

analysis, manuscript, final approval, corresponding author

Dhruv Sharma, MD, Vincent J. Campiti, BS - Experimental design, data collection, analysis, manuscript, final approval

Sarah J. Burgin, MD, Elisa A. Illing, MD, Jonathan Y. Ting, MD, MS, MBA, Park, Jae Hong, PhD, CIH, Karl R. Koehler, PhD, Hui Bae Lee, MD - Experimental design, materials acquisition, data analysis, manuscript, final approval

Dominic J. Vernon, MD, Jeffrey D. Johnson, MD, B. Ryan Nesemeier, MD - Experimental design, data collection, analysis, manuscript, final approval

Taha Z. Shipchandler, MD - Experimental design, materials acquisition, data collection, analysis, manuscript, final approval, senior author

Declaration of competing interest

The authors have no conflict of interests to disclose. This work has not been submitted for publication elsewhere.

Acknowledgements

We would like to thank Stryker Corporation (Kalamazoo, Michigan) for their generous contribution of materials and equipment for this study.

References

[1] WHO Coronavirus Disease (COVID-19) Dashboard. WHO coronavirus disease (COVID-19) dashboard. https://covid19.who.int/. [Accessed 27 September 2020].
[2] Modes of transmission of virus causing COVID-19: implications for IPC precaution recommendations. https://www.who.int/news-room/commentaries/detail/modes-of-transmission-of-virus-causing-covid-19-implications-for-ipc-precaution-recommendations. [Accessed 27 September 2020].
[3] Dbouk T, Drikakis D. On coughing and airborne droplet transmission to humans. Phys Fluids 2020;32(5):053310. https://doi.org/10.1063/5.0011960.
[4] Liu Y, Ning Z, Chen Y, et al. Aerodynamic characteristics and RNA concentration of SARS-CoV-2 aerosol in Wuhan hospitals during COVID-19 outbreak. bioRxiv March 2020. https://doi.org/10.1101/2020.03.08.982637. 2020.03.08.982637.
[5] Ong SWX, Tan YK, Chia PY, et al. Air, surface environmental, and personal protective equipment contamination by severe acute respiratory syndrome coronavirus 2 (SARS-CoV-2) from a symptomatic patient. JAMA - J Am Med Assoc. 2020;323(16):1610–1612. doi:https://doi.org/10.1001/jama.2020.3227.
[6] Diaz A, Sarac BA, Schoenbrunner AR, Janis JE, Pawlik TM. Elective surgery in the time of COVID-19. Am J Surg 2020;219(6):900–2. https://doi.org/10.1016/j.amjsurg.2020.04.014.
[7] Xie H-T, Jiang S-Y, Xu K-K, et al. SARS-CoV-2 in the ocular surface of COVID-19 patients. Eye Vis 2020;7(1):23. https://doi.org/10.1186/s40662-020-00189-0.
[8] Danesh-Meyer HV, McGhee CN. Implications of COVID-19 for ophthalmologists. Am J Ophthalmol September 2020. https://doi.org/10.1016/j.ajo.2020.09.027.
[9] Lee S, Meyler P, Mozel M, Tauh T, Merchant R. Asymptomatic carriage and transmission of SARS-CoV-2: what do we know? Can J Anesth 2020;67(10):1424–30. https://doi.org/10.1007/s12630-020-01729-x.
[10] Sun H, Wu P, Song L, Hu J, Dong S, Lu W. Clinical outcomes of early repair for open orbital fracture. Chinese J Ophthalmol. 2016;52(4):273–277. doi:https://doi.org/10.3760/cma.j.issn.0412-4081.2016.04.008.
[11] Yamanaka Y, Watanabe A, Sotozono C, Kinoshita S. Impact of surgical timing of postoperative ocular motility in orbital blowout fractures. Br J Ophthalmol 2018;102(3):398–403. https://doi.org/10.1136/bjophthalmol-2017-310312.
[12] Yu DY, Chen CH, Tsay PK, Leow AM, Pan CH, Chen CT. Surgical timing and fracture type on the outcome of diplopia after orbital fracture repair. Ann Plast Surg 2016;76:S91–5. https://doi.org/10.1097/SAP.0000000000000726.
[13] Jazayeri HE, Khavanin N, Yu JW, et al. Does early repair of orbital fractures result in superior patient outcomes? A systematic review and meta-analysis. J Oral Maxillofac Surg 2020;78(4):568–77. https://doi.org/10.1016/j.joms.2019.09.025.
[14] Jewett DL, Heinsohn P, Bennett C, Rosen A, Neuilly C. Blood-containing aerosols generated by surgical techniques: a possible infectious hazard. Am Ind Hyg Assoc J 1992;53(4):228–31. https://doi.org/10.1080/15298669291359564.
[15] Sharma D, Rubel KE, Ye MJ, et al. Cadaveric simulation of endoscopic endonasal procedures: analysis of droplet splatter patterns during the COVID-19 pandemic. Otolaryngol - Head Neck Surg (United States). 2020;163(1):145–150. doi:https://doi.org/10.1177/0194599820929274.
[16] Sharma D, Rubel KE, Ye MJ, et al. Cadaveric simulation of otologic procedures: an analysis of droplet splatter patterns during the COVID-19 pandemic. Otolaryngol - Head Neck Surg (United States). 2020;163(2):320–324. doi:https://doi.org/10.1177/0194599820930245.
[17] Workman AD, Welling DB, Carter BS, et al. Endonasal instrumentation and aerosolization risk in the era of COVID-19: simulation, literature review, and proposed mitigation strategies. Int Forum Allergy Rhinol 2020;10(7):798–805. https://doi.org/10.1002/alr.22577.
[18] Sadhu S, Agrawal R, Pyare R, et al. COVID-19: limiting the risks for eye care professionals. Ocul Immunol Inflamm 2020;28(5):714–20. https://doi.org/10.1080/09273948.2020.1755442.
[19] Ho D, Low R, Tong L, Gupta V, Veeraraghavan A, Agrawal R. COVID-19 and the ocular surface: a review of transmission and manifestations. Ocul Immunol Inflamm 2020;28(5):726–34. https://doi.org/10.1080/09273948.2020.1772313.
[20] Johnson GK, Robinson WS. Human immunodeficiency virus-1 (HIV-1) in the vapors of surgical power instruments. J Med Virol 1991;33(1):47–50. https://doi.org/10.1002/jmv.1890330110.
[21] Nogler M, Lass-Flörl C, Wimmer C, Mayr E, Bach C, Ogon M. Contamination during removal of cement in revision hip arthroplasty. A cadaver study using ultrasound and high-speed cutters. J Bone Jt Surg - Ser B. 2003;85(3):436–439. doi:https://doi.org/10.1302/0301-620X.85B3.12451.
[22] Nogler M, Lass-Flörl C, Wimmer C, Bach C, Kaufmann C, Ogon M. Aerosols produced by high-speed cutters in cervical spine surgery: extent of environmental contamination. Eur Spine J 2001;10(4):274–7. https://doi.org/10.1007/s005860100310.
[23] Makovicka JL, Bingham JS, Patel KA, Young SW, Beauchamp CP, Spangehl MJ. Surgeon personal protection: an underappreciated benefit of positive-pressure exhaust suits. Clin Orthop Relat Res 2018;476(6):1341–8. https://doi.org/10.1007/s11999.0000000000000253.
[24] Ye MJ, Sharma D, Campiti VJ, et al. Aerosol and droplet generation from mandible and midface fixation: surgical risk in the pandemic era. Am J Otolaryngol 2020;42(1):102829. https://doi.org/10.1016/j.amjoto.2020.102829.
[25] Bertroche JT, Pipkorn P, Zolkind P, Buchman CA, Zevallos JP. Negative-pressure aerosol cover for COVID-19 tracheostomy. JAMA Otolaryngol - Head Neck Surg 2020;146(7):672–4. https://doi.org/10.1001/jamaoto.2020.1081.
[26] Kim JM, Chung YS, Jo HJ, et al. Identification of coronavirus isolated from a patient in Korea with covid-19. Osong Public Heal Res Perspect 2020;11(1):3–7. https://doi.org/10.24171/j.phrp.2020.11.1.02.
[27] Neuman BW, Adair BD, Yoshioka C, et al. Supramolecular architecture of severe acute respiratory syndrome coronavirus revealed by electron cryomicroscopy. J Virol. 2006;80(16):7918–7928. doi:https://doi.org/10.1128/jvi.00645-06.
[28] David AP, Jiam NT, Reither JM, Gurrola JG, Aghi MK. El-Sayed IH. Endoscopic skull base and transoral surgery during COVID-19 pandemic: minimizing droplet spread with negative-pressure otolaryngology viral isolation drape. In: Head and neck. vol 42. John Wiley and Sons Inc.; 2020. p. 1577–82. https://doi.org/10.1002/hed.26239.
[29] Patino Montoya M, Chitilian HV. Extubation barrier drape to minimise droplet spread. Br J Anaesth 2020;125(1):e195–6. https://doi.org/10.1016/j.bja.2020.03.028.
[30] Carron JD, Buck LS, Harbarger CF, Eby TL. A simple technique for droplet control during mastoid surgery. JAMA Otolaryngol - Head Neck Surg 2020;146(7):671–2. https://doi.org/10.1001/jamaoto.2020.1064.
[31] Küçükdurmaz F, Imren Y, Akkoyunlu Y, Tuncay I, Şen C. Domestic electric drills in the service of orthopaedic surgery: a potential and preventable source of surgical site infections. Acta Orthop Traumatol Turc. 2012;46(6):455–459. doi:https://doi.org/10.3944/AOTT.2012.2794.
[32] Guderian DB, Loth AG, Weiß R, Diensthuber M, Stöver T, Leinung M. In vitro comparison of surgical techniques in times of the SARS-CoV-2 pandemic: electrocautery generates more droplets and aerosol than laser surgery or drilling. Eur Arch Oto-Rhino-Laryngology. 2020;1:3. doi:https://doi.org/10.1007/s00405-020-06330-y.
[33] Gadkaree SK, Derakhshan A, Workman AD, Feng AL, Quesnel AM, Shaye DA. Quantifying aerosolization of facial plastic surgery procedures in the COVID-19 era: safety and particle generation in craniomaxillofacial trauma and rhinoplasty. Facial Plast Surg Aesthetic Med. 2020;22(5):321–326. doi:https://doi.org/10.1089/fpsam.2020.0322.